Prediction of DP600 and TRIP780 yield loci using Yoshida anisotropic yield function

To cite this article: Iman Sari Sarraf and Daniel E Green 2018 *IOP Conf. Ser.: Mater. Sci. Eng.* **418** 012089

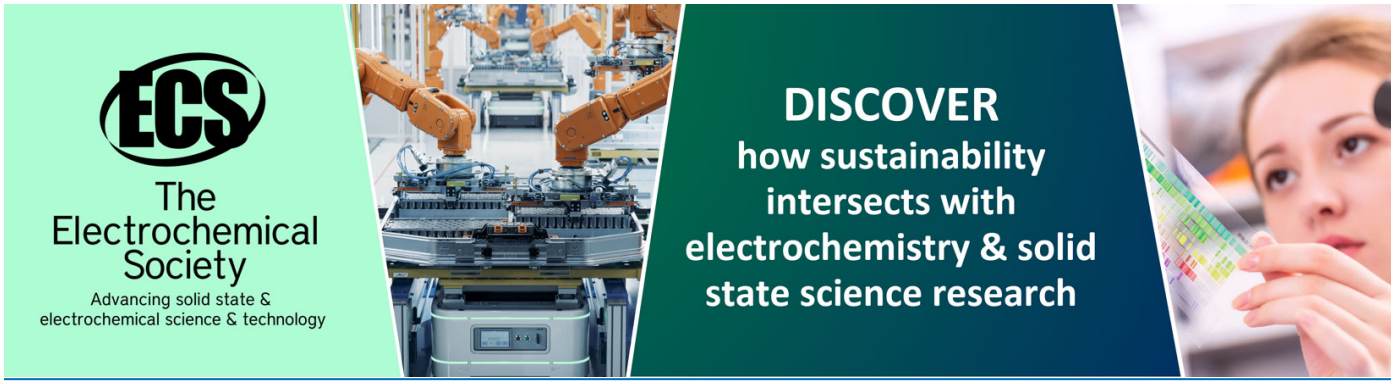

IOP Conf. Series: Materials Science and Engineering **418** (2018) 012089 doi:10.1088/1757-899X/418/1/012089

Prediction of DP600 and TRIP780 yield loci using Yoshida anisotropic yield function

Iman Sari Sarraf[1] and Daniel E Green[2]

[1,2] Department of Mechanical, Automotive, and Materials Engineering, University of Windsor, 401 Sunset Avenue, Windsor, ON, N9B 3P4, Canada

E-mail: [1]sarisa@uwindsor.ca

Abstract.
The continual demand for vehicle weight reduction, improved fuel efficiency and crashworthiness has driven the automotive industry to increasingly fabricate automotive body parts from advanced high strength steel (AHSS) sheet, such as dual phase (DP) and transformation induced plasticity (TRIP) steels. It is therefore essential to carefully investigate the forming behaviour of these sheet materials under various forming conditions. In this work, the quasi-static tensile flow behaviour of DP600 and TRIP780 sheet specimens was obtained in three orientations (RD, DD, and TD) with respect to the sheet rolling direction. A 3-parameter Voce hardening function was then fitted to each flow curve in order to determine true stress and true strain based on constant amount of plastic work per unit volume to calculate the normalized yield stress as well as the r-value for each material orientation. Yoshida's 6th-order polynomial anisotropic yield function, expressed as a function of the second and third invariants of the deviatoric stress tensor (J_2 and J_3, respectively), was used to predict the mechanical response of these two sheet materials. A new optimization method based on the Markov chain Monte Carlo (MCMC) MetropolisHastings (MH) algorithm was employed to calibrate the anisotropic yield function and determine the anisotropic coefficients. The yield loci for both materials were then derived as a function of J_2 ($\sigma = f(\tilde{J}_2)$) only, and also as a function of both J_2 and J_3 ($\sigma = f(\tilde{J}_2, \tilde{J}_3)$). The performance of each function is evaluated and validated by comparing the numerical predictions of r-value and flow stress directionality with the experimental results. And the effects of J_2 and J_3 in predicting the shape of the yield locus of DP600 and TRIP780 are also discussed.

1. Introduction

The automotive industry increasingly uses advanced high-strength steels such as dual phase (DP) and transformation induced plasticity (TRIP) steel sheets to reduce car body weight, improve fuel efficiency and increase crash safety performance. These materials demonstrate superior mechanical properties in terms of high ductility, formability, work hardening rate and strength-to-weight ratio due to their composite ferrite-martensite microstructure [1, 2]. Nevertheless, precise simulation of any sheet metal forming processes cannot be performed without considering an accurately calibrated plasticity model which describes sheet material properties and its mechanical response during deformation. Accordingly, different forming behaviour associated with the planar anisotropy and flow stress directionality results in a significant change in the prediction of flow surface shape of a material that will subsequently be employed to estimate residual stresses and numerical analysis of strain distribution along the sheet metal specimen [3, 4].

In this regard, numerous anisotropic yield functions have been developed and proposed since Hill [5], in 1948, postulated his first phenomenological quadratic anisotropic yield function using von Mises isotropic plastic potential concept. Boehler et al. [6] suggested the linear transformation of the stress tensor to determine the yield criterion. However, in 1979, Hill [7] proposed a general yield expression based on a non-quadratic yield function and subsequently developed other plane stress yield criteria [8, 9]. Barlat et al. [8] used the concept of a fourth order linear transformation operator on the stress tensor to introduce their anisotropic yield function and subsequently, a plane stress yield criteria (Yld2000-2d) [10] and an anisotropic yield function for three dimensional stress state [11] were introduced utilizing two linear transformations of the stress tensor or the deviatoric one. Hassannejadasl et al. [4] used Yld2004-18p yield function to predict flow surfaces of DP600 sheet at a wide range of strain rates (from $0.001s^{-1}$ to $1000s^{-1}$). An alternative approach was employed by Cazacu et al. [12] in which the generalization of Drucker's (1949) 3D yield criterion to orthotropy was proposed to extend isotropic yield criterion for describing any type of material symmetry by developing generalization of second and third invariants of deviatoric stress tensor, J_2 and J_3 respectively. They used this model to describe anisotropic behaviour of thin aluminium sheet specimens [13] and pressure insensitive hexagonal close packed (hcp) materials [14] in terms of both plastic strain ratio and yield locus. Yoshida et al. [3] used the same concept to develop a sixth-order polynomial type 3D yield function (with anisotropic coefficients) and evaluated the performance of the model by comparing experimental data on several types of steel sheets and predicted planar anisotropy r-values and flow stress directionalities. They called their yield function "user-friendly" since it was capable of predicting both stress directionalities and r-values, the convexity of yield function was guaranteed and parameter derivation was easily determined. However, Lou et al. [15, 16] pointed out that these models cannot differentiate the yield locus and the effect of J_3 for FCC and BCC materials; therefore, they proposed their anisotropic yield function and anisotropic ductile fracture criterion in which enough flexibility was provided by the non-associated flow rule and the summation of n-components of the anisotropic Drucker's criterion in order to predict the anisotropic behaviour and the onset of damage in both FCC and BCC materials. They validated their model by comparing the experimental and numerically predicted results on AA 6K21-IH T4 and AA2024-T351 alloys. For a broader and more comprehensive review on plastic yielding in metals and anisotropic yield functions, the authors suggest the readers to more extended review papers such as Barlat et al. [17] and Banabic et al. [18].

In the current research, a new method based on the Markov chain Monte Carlo (MCMC) algorithm is employed to determine anisotropic coefficients of 4- and 8-parameter Yoshida 3D yield function in order to describe the anisotropic behaviour steel sheets as a function of J_2 and a combination of J_2 and J_3. The effect of different parameters and the ability of each model in predicting planar anisotropy, stress directionality and the shape of yield surface for each sheet material is then discussed and evaluated by comparing numerical results and experimental data.

2. Theoretical framework

2.1. Yield function

Based on the plastic potential theory and the associated flow rule (AFR) framework, Yoshida et al. [3] described an anisotropic yield function as a sixth-order polynomial, as follows:

$$f(\boldsymbol{s}) = \frac{27}{n}\sum_{m=1}^{n}\left[\left(\tilde{J}_2^{(m)}\right)^3 - \xi_m\left(\tilde{J}_3^{(m)}\right)^2\right] = \sigma_0^6 \tag{1a}$$

where $\boldsymbol{s}$ and σ_0 are deviatoric stress tensor and uniaxial tension yield stress in the rolling direction (RD), respectively. n is a positive integer that determines the number of components in the yield function and ξ denotes a material parameter that defines the effect of J_3 on the

yield locus. The fourth-order linear transformation tensor $\boldsymbol{L}$ which extends the isotropic yield criterion to anisotropic condition is defined as $\tilde{\boldsymbol{s}}^{(m)} = \boldsymbol{L}^{(m)}\boldsymbol{\sigma}$:

$$\boldsymbol{L}^{(m)} = \frac{1}{3}\begin{bmatrix} b_m + c_m & -c_m & -b_m & 0 & 0 & 0 \\ -c_m & c_m + a_m & -a_m & 0 & 0 & 0 \\ -b_m & -a_m & a_m + b_m & 0 & 0 & 0 \\ 0 & 0 & 0 & 3g_m & 0 & 0 \\ 0 & 0 & 0 & 0 & 3h_m & 0 \\ 0 & 0 & 0 & 0 & 0 & 3k_m \end{bmatrix} \tag{1b}$$

where a_m, b_m, c_m, g_m, h_m and k_m are anisotropic coefficients and become unity in case of isotropic condition, and g_m=h_m=k_m for the plane stress case. Explicit form of the 3D yield function based on the stress tensor (σ_{ij}) for the $\tilde{J}_2$ model (when ξ=0) and for $\tilde{J}_2 - \tilde{J}_3$ model (when $\xi \neq 0$), for a single linear transformation, are given in equation (1c) and equation (1d), respectively [3].

$$f = C_1(\sigma_x - \sigma_z)^6 - 3C_2(\sigma_x - \sigma_z)^5(\sigma_y - \sigma_z) + \cdots + 27C_{16}(\tau_{xy}^2 + \tau_{yz}^2 + \tau_{zx}^2)^3 = C_1\sigma_0^6 = \sigma_0^6 \tag{1c}$$

$$f = C_1(\sigma_x - \sigma_z)^6 - 3C_2(\sigma_x - \sigma_z)^5(\sigma_y - \sigma_z) + \cdots + 27C_{16}(\tau_{xy}^6 + \tau_{yz}^6 + \tau_{zx}^6) = C_1\sigma_0^6 = \sigma_0^6 \tag{1d}$$

where $C_{1...16}$ are material parameters and are defined as a function of anisotropic coefficients (a_m, b_m, c_m, g_m), and C_1 equals unity.

2.2. Fitting procedure

In this study, the Markov chain Monte Carlo (MCMC)-Metropolis-Hastings (MH) algorithm [19] was utilized as both a fitting method and an optimization procedure to determine anisotropic coefficients in the linear transformation tensor ($\boldsymbol{L}$). In this algorithm, Monte Carlo methods is used to draw sample numbers from a specific range that is defined for each parameter where Markov chain approach is employed to generate a sequence of random variables (a_m, b_m, c_m, g_m) according to the best set of variables that are yet calculated by this method. The Metropolis-Hastings (MH) algorithm improves the performance of the Markov chain by defining a candidate range for the set of variables [20, 21]. In the first step, an initial set of parameters is determined and the initial sum of residuals ($S_{tot}(t_0)$), as shown in equation (2) is calculated based on the experimental values of the flow stresses ($\sigma_o(\alpha)$) and r-values ($r_o(\alpha)$) and the numerically predicted ones ($\sigma_p(\alpha, t_0)$ and $r_p(\alpha, t_0)$, respectively). In the next iteration, each parameter is added or subtracted by a random amount based on MCMC-MH algorithm. The error is then compared to the previously calculated error:

- $S_{tot}(t_{i+1}) < S_{tot}(t_i)$: the new set of parameters and error is considered as initial values for the next step,
- $S_{tot}(t_{i+1}) > S_{tot}(t_i)$: nothing is changed and the loop continues till finding a better set with less error or reaches the maximum number of iterations.

Sarraf et al. [22] showed that this method can be used as a fast and computationally inexpensive optimization technique.

$$S_{tot}(t_i) = W_\sigma \sum_{i=1}^{i_{max}} |\sigma_o(\alpha) - \sigma_p(\alpha, t_i)| + W_r \sum_{i=1}^{i_{max}} |r_o(\alpha) - r_p(\alpha, t_i)| \tag{2}$$

3. Experimental data

To evaluate the performance of different models with different parameters, uniaxial tension tests were carried out on DP600 and TRIP 780 sheet specimens, with a nominal thickness of 1.5mm, at quasi-static conditions in rolling, diagonal and transverse directions (RD, DD and TD, respectively). To measure the axial and width strains, A ±12.5 mm biaxial extensometer was utilized on ASTM (E8M-04) specimens. The hardening flow behaviour of these materials in each direction were determined by converting the engineering stress-strain curves obtained from the force-displacement curve to true stress-true strain values, as shown in figure 1. More details of the experimental procedures, specimens and tools for DP600 and TRIP780 are described by Rahmaan et al. [23]. Quasi-static biaxial flow stress data of DP600 and TRIP780 using biaxial viscous pressure bulge (VPB) tests were derived from Al-Nasser [1] and Hassannejadasl[24]. To determine the flow stresses (σ_α), first a 3-parameter Voce hardening function was fitted to the flow curve of DP600 and TRIP 780 at each direction, and then, the plastic work per unit volume in RD ($\int_{\varepsilon_p=0}^{0.14} \sigma_{RD} d\varepsilon_p$) was calculated. The flow stress in other directions (DD and TD) was determined based on this reference value so that σ_α can be derived based on constant plastic work instead of constant equivalent plastic strain. The normalized flow stresses at 22.5° and 67.5° were not obtained through experimental tests; they were interpolated as the average amount of normalized stresses between 0° and 45°, and 45° and 90°, respectively [25]. In addition, the slope of a linear curve that was fitted to width and longitudinal true strain data points between strain range of 0.01-0.14 was considered as r_α. Necessary normalized flow stresses and r-values for 590HSS and 980 Y HSS were derived from Yoshida et al. [3]. Table 3 shows the experimental data that are used as the input values to calibrate the anisotropic yield function.

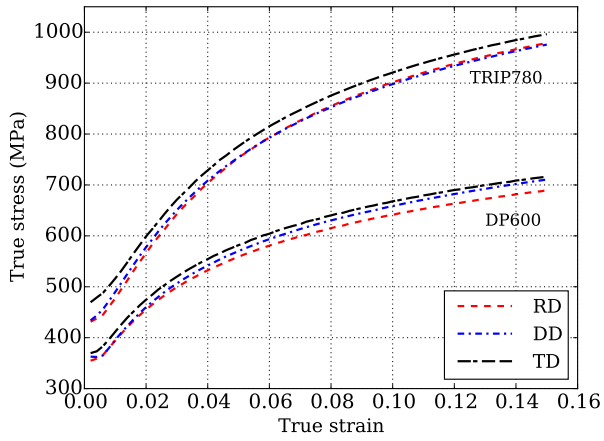

Figure 1. Quasi-static flow curves of DP600 and TRIP780 in RD, DD and TD.

Table 1. Experimental data used to calibrate Yoshida anisotropy model. (N.b. input data for 590HSS and 980 Y HSS were derived from Yoshida et al. [3].)

Material	σ_0	$\sigma_{22.5}$*	σ_{45}	$\sigma_{67.5}$*	σ_{90}	σ_b	r_0	r_{45}	r_{90}
DP600	1.000	1.014	1.028	1.035	1.041	1.076	0.646	0.896	0.853
TRIP780	1.000	0.998	0.996	1.008	1.020	1.051	0.498	1.030	0.565
590 HSS [3]	1.000	0.970	0.936	1.000	1.047	1.000	0.430	1.0410	0.610
980 Y HSS [3]	1.000	1.001	1.011	1.012	1.023	1.010	0.730	0.910	0.810

* Interpolated value.

4. Results and discussion

According to equations (1a), (1b) and (2), there are three important parameters that have direct and great effects on the prediction of both anisotropic coefficients (a_m, b_m, c_m and g_m) and material parameters ($C_{1...16}$): **(a)** weighting ratio (W_σ/W_r), **(b)** the material constant that represent the effect of J_3 (ξ) and **(c)** n which provides enough flexibility for the yield function to describe the sheet anisotropy. Since these yield functions that are developed based on the linear transformation of the stress tensor in order to predict both planar anisotropy r-values and flow stress directionality and guarantee the convexity of the yield locus, accurate selection of weighting ratio becomes essential to define a yield function more based either on stresses, r-values or a balance between both. It can be seen from figure 2 that even without the effect of J_3 (ξ=0) and n=2, i.e. 8 anisotropic coefficients: $a_1 \dots g_1$ and $a_2 \dots g_2$, when W_σ/W_r is greater than 3, the stress directionality can precisely be predicted but no agreement can be observed between experimental and predicted r-values. On the other hand, increasing W_r results in better prediction of r-values but imprecise estimation of σ_α. The shape of the yield locus changes as weighting ratio changes. Therefore, a parametric study should be carried out on a wide range of W_σ/W_r to achieve the best weighting ratio that can predict both flow stresses and r-values at each and every direction.

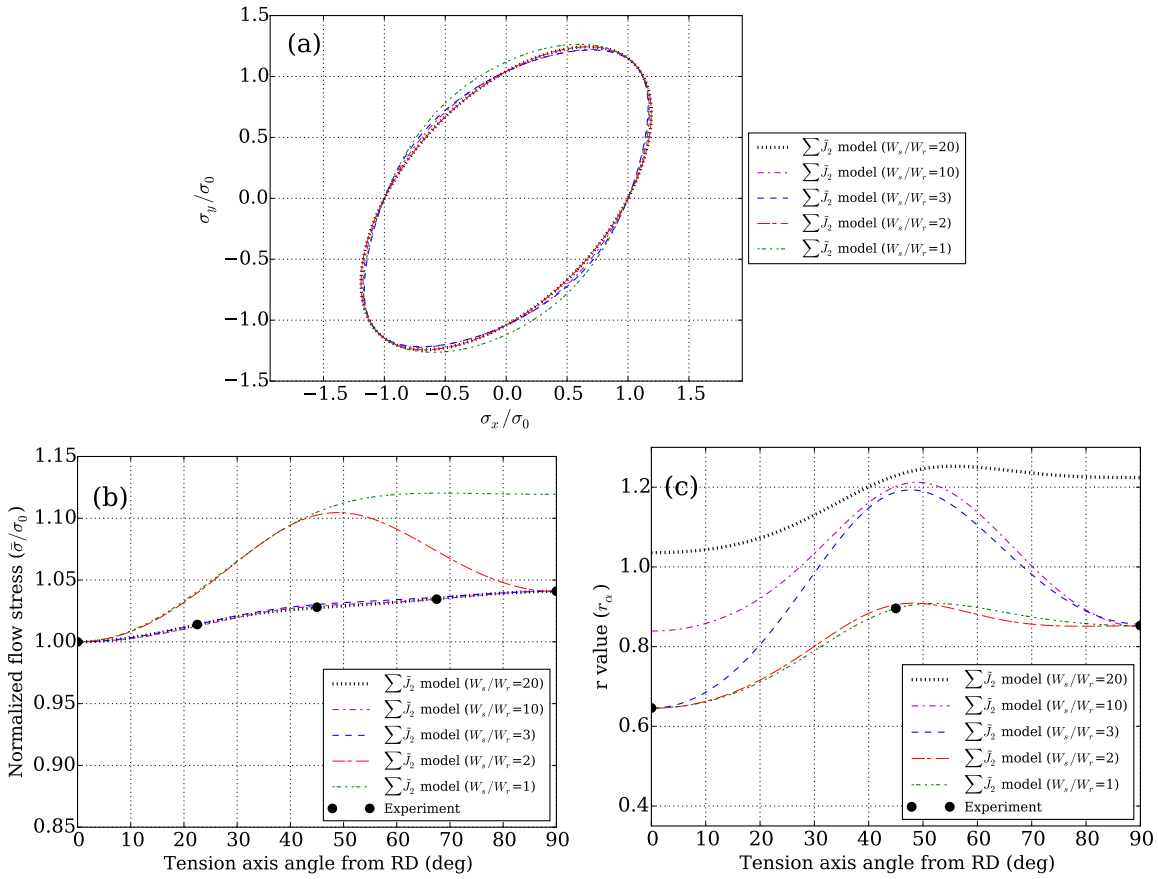

Figure 2. predicted (a) yield loci, (b) normalized flow stress and (c) r-value for DP600 using $\sum\tilde{J}_2$ and various weighting ratios.

In this research, MCMC-MH algorithm is used to determine the anisotropic parameters and

coefficients based upon 4 possible arrangements of parameters: **(a)** n=1 and n=2, and **(b)** ξ=0 and $\xi \neq 0$. To simplify the comparison between different models, W_σ/W_r=3 is considered as the constant weighting ratio. The numerically determined material parameters ($C_{1...16}$) and anisotropic coefficients (a_m, b_m, c_m and g_m, m=1,2) for the investigated sheet materials are given in table 2. Comparing the parameters obtained for 590HSS (ξ=0) and 980 Y HSS by Yoshida et al. [3] and those indicated in table 2 clearly shows that although the $C_{1...16}$ are somewhat the same for each sheet material, the anisotropic coefficients are noticeably different from each other. Therefore, it can be claimed that material parameters are unique for each material considering a specific set of values for n and ξ but ($a_m \dots g_m$ are not, i.e. same material parameters can be obtained from different anisotropic coefficients. Figure 3 shows the overall comparison of accuracy for each prediction method (N-R [3] and MCMC-MH) using equation (2). It can be seen that using MSMS-MH could significantly decrease the total error in case of 590 HSS (ξ=0) and 980 Y HSS ($\xi \neq 0$). Accordingly, the proposed optimization technique can be effectively utilized to find the global minimum error and accurately determine fitting parameters.

Table 2. Material parameters and anisotropic coefficients of Yoshida's 3D yield function (n=2).

	ξ	Material parameters and anisotropic coefficients								
DP600	0	$C_{1...8}$	1.000	0.7846	0.6433	0.6283	0.6545	0.7256	0.7863	0.8531
		$C_{9...16}$	0.7657	0.7024	0.7487	0.7884	0.8323	0.8381	0.8136	0.9108
		a_n, b_n, c_n, g_n	-0.9083	1.6572	0.2779	0.8229	1.6567	-1.7788	0.3644	-1.0712
	-1.2	$C_{1...8}$	1.000	0.7837	0.6043	0.5177	0.5638	0.7261	0.7890	0.7351
		$C_{9...16}$	0.3888	0.5972	0.8367	0.8198	0.9505	1.0929	0.8164	0.7087
		a_n, b_n, c_n, g_n	1.2187	-1.9355	0.8761	1.057	-0.3247	1.5246	0.3509	-0.5329
TRIP780	0	$C_{1...8}$	1.000	0.6648	0.4820	0.4419	0.4959	0.6414	0.8887	0.8979
		$C_{9...16}$	0.6817	0.6012	0.6724	0.8611	0.9193	0.8401	0.9035	1.1309
		a_n, b_n, c_n, g_n	0.4284	-1.5361	-0.5524	-0.9212	2.0484	-1.2947	-0.3228	1.0849
	-0.8	$C_{1...8}$	1.000	0.6631	0.5484	0.5378	0.5404	0.6411	0.8878	0.8356
		$C_{9...16}$	0.4757	0.3762	0.5216	0.8296	1.0102	1.1322	0.9872	0.9233
		a_n, b_n, c_n, g_n	-1.12	1.875	0.0845	-0.9589	-1.8021	1.3363	-0.1708	-1.0113
590 HSS	0	$C_{1...8}$	1.000	0.6014	0.4900	0.4416	0.4868	0.5740	0.7568	0.9835
		$C_{9...16}$	0.7154	0.7248	0.7781	0.9947	1.1966	1.0976	1.3409	1.8764
		a_n, b_n, c_n, g_n	1.9008	-1.3019	-0.1362	-1.1906	0.9573	-2.0481	0.3392	0.9834
	-0.8	$C_{1...8}$	1.000	0.5989	0.4830	0.3760	0.4168	0.5765	0.7592	0.8388
		$C_{9...16}$	0.3482	0.5481	0.8306	1.0574	1.3712	1.5829	1.5021	1.7973
		a_n, b_n, c_n, g_n	1.504	-1.3119	0.5078	1.1716	-0.8307	2.1317	-0.5739	1.0014
980 Y HSS	0	$C_{1...8}$	1.000	0.8434	0.7496	0.7205	0.7478	0.7800	0.8713	0.9341
		$C_{9...16}$	0.8291	0.7881	0.7819	0.8592	0.9166	0.8456	0.8617	0.9336
		a_n, b_n, c_n, g_n	0.707	-1.4116	-0.4048	0.7772	2.1936	-0.981	-1.0932	-1.0867
	-0.5	$C_{1...8}$	1.000	0.8437	0.8265	0.7795	0.7408	0.7827	0.8738	0.8782
		$C_{9...16}$	0.5764	0.6357	0.7693	0.8742	0.9882	1.0445	0.9108	0.8335
		a_n, b_n, c_n, g_n	1.6277	-1.875	0.4354	-1.0526	-0.8694	1.8848	-0.3098	0.8212

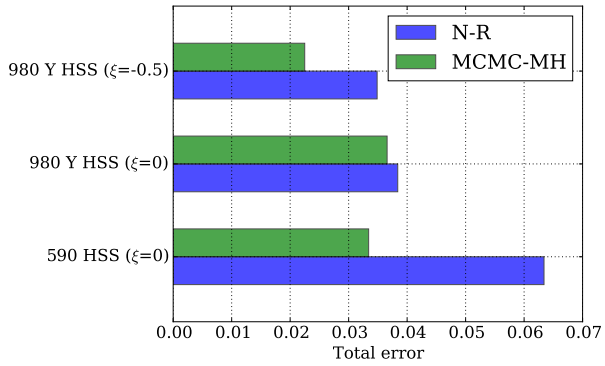

Figure 3. Comparison of accuracies between NewtonRaphson procedure (N-R) [3] and MCMC-MH method.

The effect of the number of anisotropic coefficients (n=1: $a_1 \dots g_1$ and n=2: $a_1 \dots g_2$) and ξ on the prediction of flow stress directionality is shown in figure 4. Interestingly, all models could predict stress directionality of sheet materials in an acceptable range although some of them showed better performances. In case of DP600 and TRIP780, f($\tilde{J}_2$) with $n = 2$ and f($\tilde{J}_2, \tilde{J}_3$) with n=1 showed the best prediction, however, f($\tilde{J}_2, \tilde{J}_3$) with n=2 and $\xi \neq 0$ showed a small amount of deviation from experimental results around α=45°. It is worth noting that using the latter model changed the shape of the predicted stress directionality curve for DP600, TRIP780, and 980 Y HSS.

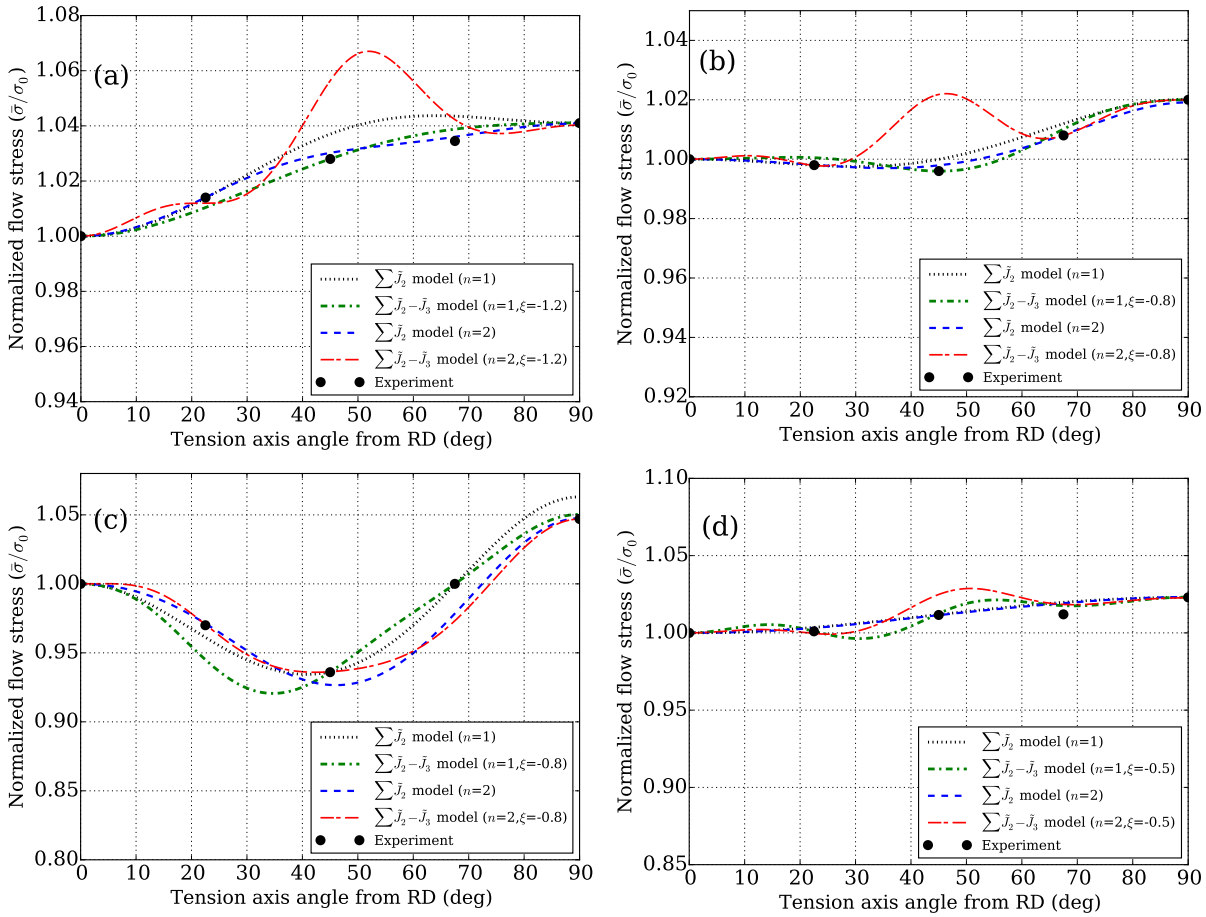

Figure 4. Measured and predicted normalized flow stress for (a) DP600, (b) TRIP780, (c) 590HSS and (d) 980 Y HSS.

The same comparison can be carried out to evaluate the ability of different models to predict planar anisotropy r-values for different sheet specimens. According to figure 5, neither f($\tilde{J}_2$) nor f($\tilde{J}_2, \tilde{J}_3$) with only four anisotropic coefficients (n=1) are capable of predicting planar anisotropy of the steel sheet specimens. On the contrary, employing more coefficients provides the models with enough flexibility to achieve better performances and including J_3 in the yield function contributes to significantly improved predictions. Nevertheless, as mentioned at the beginning of this section, ξ is an important material constant that determines the effect of J_3 in the yield function and is shown to be between -27/8$\leq$ ξ $\leq$9/4 [3, 12] in order to satisfy the convexity of the yield locus. Therefore, a comprehensive parametric study was carried out on the whole range of ξ to obtain the best fit in terms of both r-values and stress directionalities. It is worth noting that the proposed MCMC-MH algorithm tends to find the global minimum error based on the experimental results, however, with an insufficient number of data points, it is difficult to determine the true anisotropic behaviour of the material between RD, DD and TD.

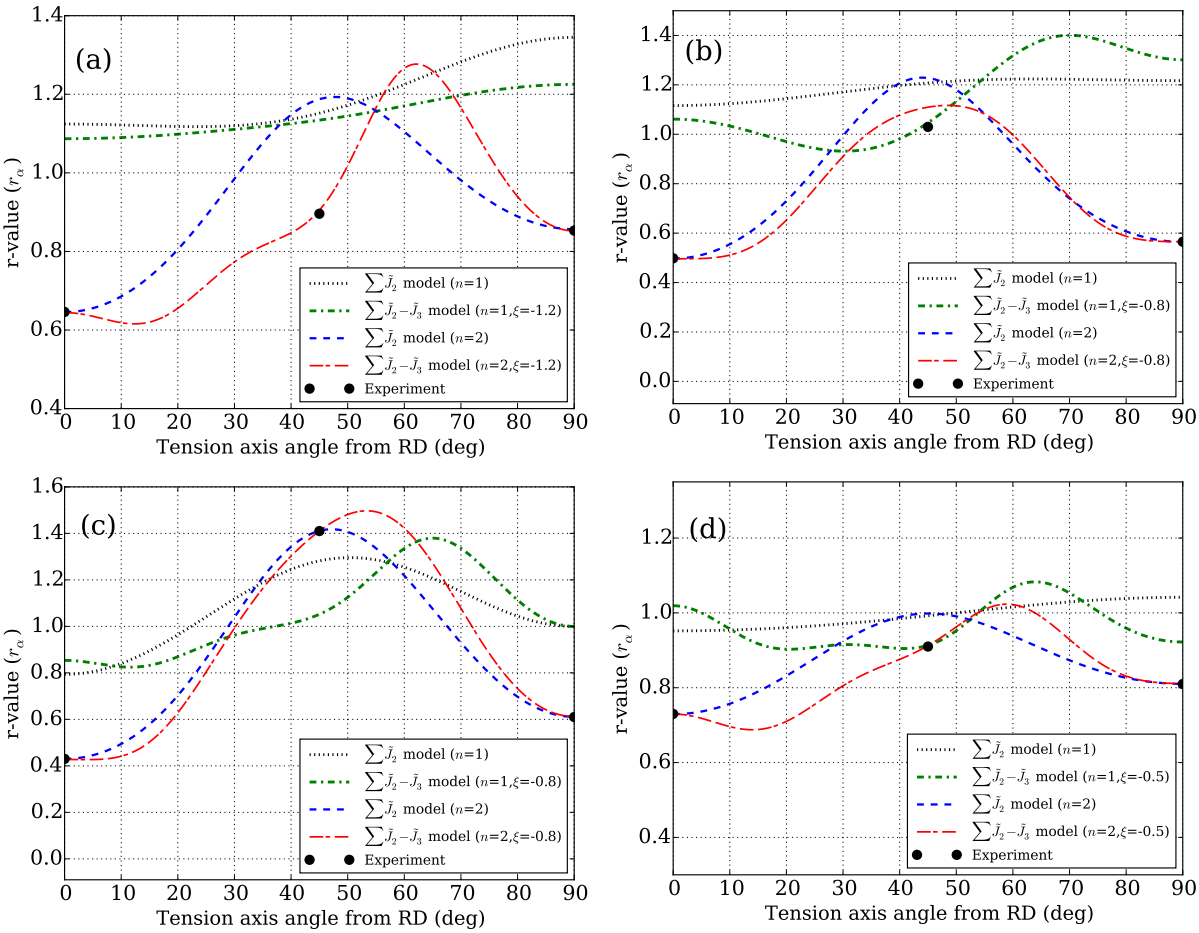

Figure 5. Measured and predicted r-values for (a) DP600, (b) TRIP780, (c) 590HSS and (d) 980 Y HSS.

The accuracy of the Yoshida anisotropic model and the proposed optimization algorithm in predicting the normalized biaxial flow stresses is shown in figure 6. It can be seen that σ_b was predicted accurately for all investigated materials since the absolute error in each case did not exceed 0.0004, however, the overall accuracy of the predictions was significantly improved for DP600, 590HSS and 980Y HSS when n=2 was used compared to n=1, with absolute errors less

than approximately 5×10^{-5}. The absolute error in calculating σ_b for TRIP780 was also reduced from ~0.0004 to less than 0.0003 when including $\tilde{J}_3$ and n=2 in the anisotropic yield function. Generally, the effect of $\tilde{J}_3$ becomes significant when determining σ_b; and the same effect can be observed in figure 6 where the accuracy of predictions was increased in all cases, except for 980Y HSS (n=1).

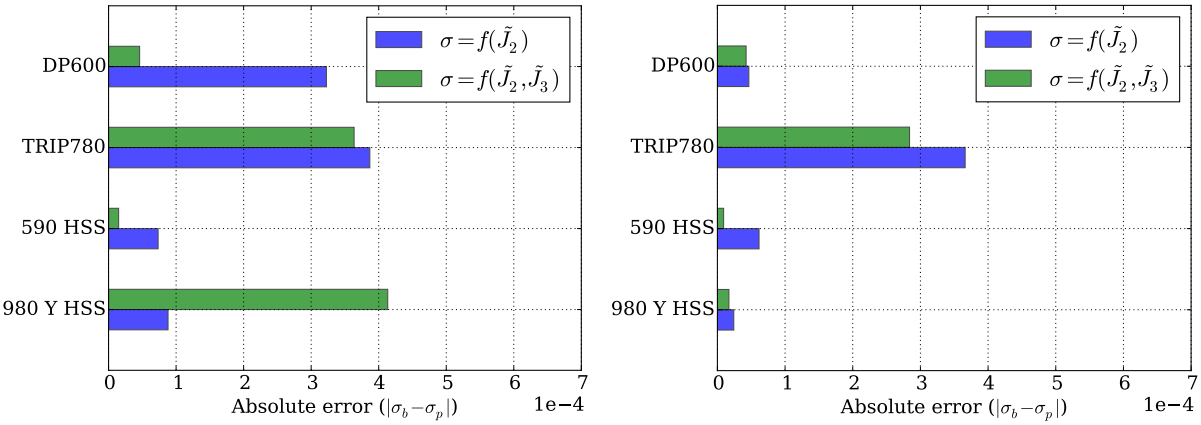

Figure 6. Comparison of absolute error in predicting normalized biaxial stress when n=1 (left) and n=2 (right).

Quasi-static yield loci for all four steel sheet materials are derived by different models and sets of parameters, and expressed in 2D plane of σ_x-σ_y stress space which is shown in figure 7. Apart from 980 Y HSS (figure 7d) in which no apparent difference can be detected between different loci since all functions showed somehow the same prediction levels of σ_α(figure 4d), it can be seen that using 8 anisotropic coefficients both for f($\tilde{J}_2$) and f($\tilde{J}_2, \tilde{J}_3$) results in the similar shape of yield loci. The main difference between models with n=1 and those with n=2 can be observed in the vicinity of plane strain and simple shear regions where the ability of each function in predicting r-values is quite different. As shown in figures 4 and 6, all models with different arrangement of parameters are capable of predicting σ_α and σ_b with an acceptable accuracy, but those with n=1 were not able to predict r-values which is the main factor to determine the shape of yield locus in the shear and plane-strain regions. The predicted yield surfaces for 590HSS and 980 Y HSS using $\tilde{J}_2$ and $\tilde{J}_2$-$\tilde{J}_3$ models with n=2 are in very good agreement with experimental and numerical results obtained via N-R method by Yoshida et al. [3].

5. Summary and conclusions

Anisotropic behaviour of four different high strength steel sheet specimens are evaluated using a sixth-order polynomial yield function that can describe both stress directionality (σ_α) and planar anisotropy (r_α). The proposed MCMC-MH procedure is easy to implement in a programming environment and can effectively be used to determine the anisotropic coefficients in the model to obtain the minimum total error. Nevertheless, more experimental data points are needed to determine the true anisotropic behaviour of the material between RD, DD and TD.

In Yoshida's proposed anisotropic function, three parameters are identified as important components to define the behaviour and performance of the yield function. The first one is the number of anisotropic parameters ($a_m \dots g_m$, $m = 1 \dots n$) where n=1 and n=2 result in 4 and 8 anisotropic coefficients, respectively. It is shown that although both $\tilde{J}_2$ model and $\tilde{J}_2 - \tilde{J}_3$ model with n=1 can describe the stress directionalities within an acceptable range; However, they can hardly predict the r-values of the sheet materials. Therefore, n=2 is recommended

to establish an accurate linear transformation tensor. The second parameter that needs to be carefully determined through a parametric study, is the weighting ratio between flow stresses and planar anisotropy (W_σ/W_r) in which the anisotropic yield can change from stress based to r-value based by decreasing this ratio. A weighting ratio of 3 is found to establish a reasonable balance between the accuracy of predicting both stress directionalities and planar anisotropies. The last parameter that determines the behaviour of the yield function is ξ which defines the presence and the effect of $\tilde{J}_3$ in the model. Despite the fact that $\tilde{J}_2$ model can capture the anisotropic behaviour of the investigated steels with an acceptable precision, taking $\tilde{J}_3$ into account can considerably improve the ability of the yield function particularly in predicting r-values. Therefore, it can be assumed that $\tilde{J}_2-\tilde{J}_3$ model can be a better choice when dealing with materials with higher number of data points and more complex anisotropic behaviour. However, a comprehensive parametric study should be carried out on the wide range of ξ to select the best fitting value for this material constant.

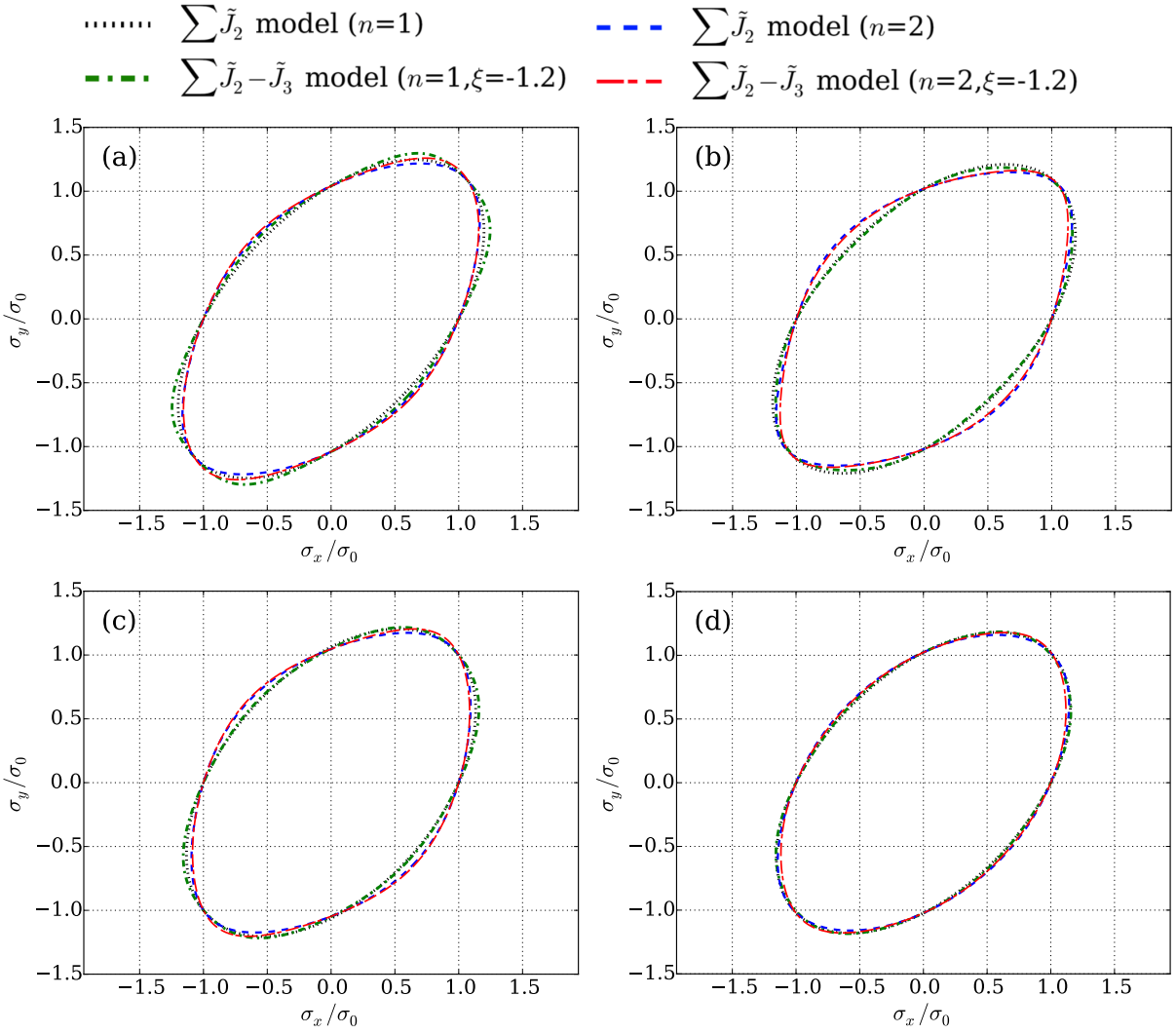

Figure 7. Predicted yield loci by Yoshida anisotropy model for (a) DP600, (b) TRIP780, (c) 590HSS and (d) 980 Y HSS.

Acknowledgments
This work was funded by NSERC-Automotive Partnership Canada (APCPJ 418056-11) program and supported by ArcelorMittal Dofasco, CanmetMATERIALS-Natural Resources Canada, Ford Research & Advanced Engineering, Novelis Inc. and Amino N.A. Corp. The authors gratefully acknowledge ArcelorMittal-Dofasco for supplying the DP600 and TRIP780 sheet materials used in this research.

References

[1] Nasser A, Yadav A, Pathak P and Altan T 2010 *Journal of Materials Processing Technology* **210** 429–436 ISSN 09240136
[2] Uthaisangsuk V, Prahl U and Bleck W 2011 *Engineering Fracture Mechanics* **78** 469–486 ISSN 00137944
[3] Yoshida F, Hamasaki H and Uemori T 2013 *International Journal of Plasticity* **45** 119–139 ISSN 07496419
[4] Hassannejadasl A, Rahmaan T, Green D E, Golovashchenko S F and Worswick M J 2014 *Procedia Engineering* **81** 1378–1383 ISSN 18777058
[5] Hill R 1948 A theory of the yielding and plastic flow of anisotropic metals *Proc. R. Soc. Lond. A* vol 193 (The Royal Society) pp 281–297
[6] Boehler J P and Sawczuk A 1970 *J. Mécanique* **9** 5–33
[7] Hill R 1979 Theoretical plasticity of textured aggregates *Mathematical Proceedings of the Cambridge Philosophical Society* vol 85 (Cambridge University Press) pp 179–191
[8] Hill R 1990 *Journal of the Mechanics and Physics of Solids* **38** 405–417
[9] Hill R 1993 *International Journal of Mechanical Sciences* **35** 19–25
[10] Barlat F, Brem J C, Yoon J W, Chung K, Dick R E, Lege D J, Pourboghrat F, Choi S H and Chu E 2003 *International Journal of Plasticity* **19** 1297–1319
[11] Barlat F, Aretz H, Yoon J W, Karabin M E, Brem J C and Dick R E 2005 *International Journal of Plasticity* **21** 1009–1039
[12] Cazacu O and Barlat F 2001 *Mathematics and Mechanics of Solids* **6** 613–630 ISSN 1081-2865 (*Preprint* 0803973233)
[13] Cazacu O and Barlat F 2003 *International Journal of Engineering Science* **41** 1367–1385 ISSN 00207225
[14] Cazacu O and Barlat F 2004 *International Journal of Plasticity* **20** 2027–2045 ISSN 07496419
[15] Lou Y and Yoon J W 2017 *Procedia Engineering* **207** 233–238
[16] Lou Y and Yoon J W 2018 *International Journal of Plasticity* **101** 125–155
[17] Barlat F, Cazacu O, Banabic D, Yoon J W and Others 2004 *Continuum scale simulation of engineering materials: fundamentals-microstructures-process applications* 145–183
[18] Banabic D, Barlat F, Cazacu O and Kuwabara T 2010 *International Journal of Material Forming* **3** 165–189 ISSN 19606206
[19] Andrieu C, De Freitas N, Doucet A and Jordan M I 2003 *Machine Learning* **50** 5–43 ISSN 08856125 (*Preprint* 1109.4435v1)
[20] Mathew M 2013 *The application of Markov chain Monte Carlo techniques in non-linear parameter estimation for chemical engineering models* Ph.D. thesis University of Waterloo
[21] Han X L, Pozdin V, Haridass C and Misra P 2006 *Journal of Information & Computational Science* **3** 1–7 ISSN 15487741
[22] Sarraf I S, Jenab A, Boyle K P and Green D E 2017 *Materials & Design* **117** 267–279 ISSN 02641275
[23] Rahmaan T, Bardelcik A, Imbert J, Butcher C and Worswick M J 2016 *International Journal of Impact Engineering* **88** 72–90 ISSN 0734743X
[24] Hassannejadasl A 2014 *Simulation of electrohydraulic forming using anisotropic, rate-dependent plasticity models* Ph.D. thesis University of Windsor
[25] Hu W 2007 *International Journal of Plasticity* **23** 620–639 ISSN 0749-6419